MERIS AND THE RED-EDGE INDEX

J.G.P.W. Clevers, S.M. De Jong, G.F. Epema, E.A. Addink
Centre for Geo-Information (CGI)
Wageningen-UR
P.O. Box 47
NL-6700 AA Wageningen, The Netherlands
E-mail: jan.clevers@staff.girs.wag-ur.nl

F. Van Der Meer, W.H. Bakker, A.K. Skidmore
ITC
P.O. Box 6
NL-7500 AA Enschede, The Netherlands

KEY WORDS: Red-edge, Sensitivity Analysis, MERIS, Imaging Spectrometry

ABSTRACT

Within ESA's Earth Observation programme, the Medium Resolution Imaging Spectrometer (MERIS) is one of the payload components of the European polar platform ENVISAT-1. MERIS will be operated with a standard band setting of 15 bands. Data will be acquired at 300 m spatial resolution over land, thus vegetation monitoring can be performed at regional to global scales. The objectives of this paper are: (1) to study which factors determine the vegetation red-edge index, (2) to study whether this red-edge index can be derived from the MERIS standard band setting, and (3) to show what such a red-edge index means at the scale level of MERIS data.. Two different data sets are explored for simulating the red-edge using MERIS spectral bands: (1) simulated data using reflectance models, and (2) airborne reflectance spectra of an agricultural area obtained from AVIRIS. Results show that a "linear method", assuming a straight slope of the reflectance spectrum around the midpoint of the slope, is a robust method for determining the red-edge position. Results also show that the MERIS bands at 665, 705, 753.75 and 775 nm can be used for applying the "linear method" for red-edge index estimation. Results of the translation to the MERIS' scale are also presented.

1. INTRODUCTION

The spectral signature of living plant material is dominated by chlorophyll, the cell structure and the water content, which influence the amount of reflected radiation in the VIS, NIR and SWIR region of the electromagnetic spectrum. Imaging spectrometers offer new possibilities to estimate, for instance, important carbohydrates of plants from the reflected radiation of vegetation (Elvidge, 1990). However, at present the remote sensing of foliar chemical concentrations, other than chlorophyll and water, has not been very successful. The presence of water in living leaf tissue almost completely masks these biochemical absorption features. Recently, Clevers (1999) showed that imaging spectrometry might provide additional information at the red-edge region, not covered by the information derived from a combination of a NIR and a VIS broad spectral band. He concluded that, concerning high spectral resolution data, this seems to be the major contribution of imaging spectrometry to applications in agriculture.

The region of the red-edge concerns the region of the sharp rise in reflectance of green vegetation between 670 and 780 nm, which can be used for studying the chlorophyll content as a measure of plant condition (Horler *et al*., 1983). Both the position and the slope of the red-edge change under stress conditions, resulting in a shift of the slope towards shorter wavelengths (e.g. Horler *et al*., 1983, Wessman, 1994). The position of the red-edge is defined as the position of the main inflexion point of the red-NIR slope. This is often also denoted as the red-edge index.

Within ESA's Earth Observation programme, MERIS (Medium Resolution Imaging Spectrometer) will be one of the main payload components of the European polar platform ENVISAT-1 to be launched in 2001 (ESA, 1997). MERIS is a 15 band, programmable imaging spectrometer, which allows for changes in band position and bandwidths throughout its lifetime. It is designed to acquire data at variable bandwidth of 1.25 to 30 nm over the spectral range of 390 – 1040 nm. Band choice and bandwidth depend on the width of the spectral feature observed and the amount of energy needed in a band for adequate observation (Rast and Bezy, 1990). Data will be acquired at 300 m spatial resolution over land, thus vegetation monitoring can be performed at regional to global scales. MERIS will be operated with a standard band setting (as shown in table 1). However, it has the capability of in-flight selection of bands for specific applications or

experiments, for repositioning of bands because of new findings or to cope with partial instrument failures or deficiencies, and for exploration of new issues. Operational constraints, however, will limit the number and frequency of band changes.

Table 1. The 15 spectral bands of the standard band setting for MERIS (Rast et al., 1999).

Band nr.	Band centre [nm]	Bandwidth [nm]
1	412.5	10
2	442.5	10
3	490	10
4	510	10
5	560	10
6	620	10
7	665	10
8	681.25	7.5
9	705	10
10	753.75	7.5
11	760	2.5
12	775	15
13	865	20
14	890	10
15	900	10

The best MERIS resolution of 300 m should be sufficient to monitor the highly heterogeneous terrestrial surfaces at scales required for global change studies (ESA, 1995, Verstraete *et al*., 1999). Vegetation indices using red and NIR reflectance can be used for estimating the LAI and the fraction of absorbed photosynthetically active radiation (Govaerts *et al*., 1999). The red-edge feature may provide useful information on the physiological status of the vegetation under observation. Verstraete *et al*. (1999) noted that the spectral and spatial resolution of MERIS will be particularly appropriate to derive this red-edge variable. However, they also state that much research is needed to design algorithms based on MERIS data. The first objective of this paper is to study which vegetation and external variables determine the red-edge index. The second and main objective is to study whether the red-edge index can be derived from the MERIS standard band setting, as this will be the setting that will be applied under normal operation. In this study we will also pay some attention to the interpretation and application of a red-edge index at the spatial scale MERIS is operating at.

2. METHODOLOGY FOR DETERMINING THE RED-EDGE INDEX

Since the position of the red-edge is defined as the inflexion point (or maximum slope) of the red infrared slope, an accurate determination requires a number of spectral measurements in narrow bands in this region. Subsequently, the red-edge position is defined by the maximum first derivative of the reflectance spectrum in the region of the red-edge. High-order curve fitting techniques are employed to fit a continuous function to the derivative spectrum (Horler *et al*., 1983, Demetriades-Shah and Steven, 1988, Demetriades-Shah *et al*., 1990). However, existing curve fitting techniques are complex. Recently, Dawson and Curran (1998) presented a technique based upon a three-point Lagrangian interpolation technique for locating the red-edge position in spectra that have been sampled coarsely. A problem with this method arises when the reflectance spectrum exhibits more than one maximum in its first derivative. Horler *et al*. (1983) identified two components in the first derivative spectrum with peaks around 700 and 725 nm. The red-edge index then represented whichever component was dominant, and therefore a red-edge shift could involve a jump between the two components, creating a discontinuity in the red-edge index. They found that the second component moves to longer wavelengths and becomes more pronounced as the LAI increases.

For practical reasons, fitting a curve to a few measurements in the red-edge region (requiring an instrument with not so many spectral bands) often is applied for approximating the inflexion point. First, a polynomial function may be fitted to the data (Clevers and Büker, 1991). Secondly, a so-called inverted Gaussian fit to the red infrared slope may be applied (Bonham-Carter, 1988). Finally, Guyot and Baret (1988) applied a simple linear model to the red infrared slope. A comparison of the three methods yielded comparable results (Clevers and Büker, 1991, Büker and Clevers, 1992). Since the method of Guyot and Baret (1988) uses only four wavelength bands, this method is likely to be applicable to

future sensors. Moreover, Clevers et al. (2000) found for various data sets that the latter method is much more robust than procedures based on the first derivative spectrum because the first derivative spectrum did not have one unique maximum. Therefore it was chosen to use the method of Guyot and Baret for this study.

The linear interpolation as described by Guyot and Baret (1988) assumes that the reflectance curve at the red-edge can be simplified to a straight line centred around a midpoint between the reflectance in the NIR at about 780 nm and the reflectance minimum of the chlorophyll absorption feature at about 670 nm. These authors estimated the reflectance value at the inflexion point and applied a linear interpolation procedure for the measurements at 700 and 740 nm estimating the wavelength corresponding to the estimated reflectance value at the inflexion point. Here we refer to this method as the "linear method", which can be described in the following way:

(1) Calculation of the reflectance at the inflexion point (R_{re}):

$$R_{re} = (R_{670} + R_{780})/2 \quad (1)$$

(2) Calculation of the red-edge wavelength (λ_{re}):

$$\lambda_{re} = 700 + 40 * ((R_{re} - R_{700})/(R_{740} - R_{700})) \quad (2)$$

R_{670}, R_{700}, R_{740} and R_{780} are the reflectance values at 670, 700, 740 and 780 nm wavelength, respectively, and the constants 700 and 40 result from interpolation in the 700 – 740 nm interval.

3. DATA SETS

Two different data sets will be used.

(I) Simulated data with a combination of the PROSPECT leaf reflectance model and the SAIL canopy reflectance model;

(II) Airborne reflectance spectra of agricultural crops obtained from AVIRIS.

Jacquemoud and Baret (1990) developed a leaf model that simulates leaf reflectance and leaf transmittance as a function of leaf properties: the PROSPECT model. The PROSPECT model is a radiative transfer model for individual leaves based on the generalised "plate model" of Allen *et al*. (1969, 1970). The model considers a compact theoretical plant leaf (without air cavities) as a transparent plate with rough plane parallel surfaces. An actual leaf is assumed to be composed of a pile of N homogeneous compact layers separated by N-1 air spaces. The compact leaf (N = 1) has no intercellular air spaces or the intercellular air spaces of the mesophyll have been infiltrated with water. The discrete approach can be extended to a continuous approach where N needs not be an integer value. PROSPECT allows computing the 400-2500 nm reflectance and transmittance spectra of different leaves using three input variables: the leaf mesophyll structure parameter N, the pigment content and the water content. All three variables are independent of wavelength. The output of the PROSPECT model can be used as input into the SAIL model.

The one-layer SAIL radiative transfer model (Verhoef, 1984) simulates canopy reflectance as a function of canopy parameters (leaf reflectance and transmittance, LAI and leaf angle distribution), soil reflectance, ratio diffuse/direct irradiation and solar/view geometry (solar zenith angle, zenith view angle and sun-view azimuth angle). Bunnik (1978) and Verhoef and Bunnik (1981) give leaf inclination distribution functions used with the SAIL model. The SAIL model has been used in many studies and validated with various data sets (e.g., Goel, 1989).

Airborne reflectance spectroscopic data used in this study were derived from the airborne visible-infrared imaging spectrometer (AVIRIS). The ER-2 aircraft of NASA, carrying AVIRIS, performed a successful flight over the Flevoland test site on July 5th, 1991 (being the middle of the growing season). AVIRIS acquires 224 contiguous spectral bands from 410 to 2450 nm. Both the spectral resolution and the spectral sampling interval are about 10 nm. However, spectral data were available only in the 400 nm to 1860 nm wavelength range because of malfunctioning of the D-spectrometer. The ground resolution is 20 m at an operating altitude of 20 km.

The preprocessing which includes correction for dark current, vignetting and radiometric response was done by the Jet Propulsion Laboratory (JPL). Atmospheric correction was also performed by JPL with a new version of the LOWTRAN 7 atmospheric model, yielding surface reflectances (Van Den Bosch and Alley, 1990). AVIRIS radiance as well as reflectance data are used in this study.

The test site was located in Southern Flevoland in The Netherlands, an agricultural area with homogeneous soils reclaimed from the lake IJsselmeer in 1966. The test site comprised ten different agricultural farms, each 45 to 60 ha in size. Main crops were sugar beet, potato and winter wheat. Regular field measurements were collected.

4. RESULTS AND DISCUSSION

4.1 Sensitivity Analysis

One of the interesting features of the red-edge index is that it seems to be independent of soil reflectance. Moreover, the atmosphere seems to have only a minor influence on the position of the red-edge. Both the soil background and the atmospheric influence hamper the use of solely one spectral band in the visible part of the spectrum for estimating leaf chlorophyll content (leaf nitrogen). In this section a sensitivity analysis is described using theoretical leaf and canopy reflectance models in order to study the influence of leaf and canopy variables and of external variables on the relationship between red-edge index and leaf chlorophyll content. The atmospheric influence on the red-edge index will also be given attention.

In this study, simulations are performed for a so-called standard crop under standard irradiation and viewing conditions, unless otherwise indicated, using a combined PROSPECT + SAIL model. The inputs for this standard crop are:

chlorophyll content of 34.24 $\mu g.cm^{-2}$ } example of a dicotyledonous plant as
N parameter of 1.8320 } given by Jacquemoud and Baret
water content of 0.0137 cm } (1990)
leaf area index (LAI) of 4
spherical leaf angle distribution (LAD)
hot-spot size parameter of 0
soil reflectance of 20%
only direct solar irradiation
solar zenith angle of 45^o
nadir viewing.

The effect of changing one input variable at a time is studied. All simulations will be restricted to vertical viewing. Clevers and Verhoef (1993) studied the influence of the observation geometry on red and NIR reflectances. They concluded that off-nadir viewing effects become significant at angles larger than about 7 degrees (and most pronounced in the direction of the hot spot). So, in this study we did not investigate the influence of off-nadir viewing on the relationship between red-edge index and chlorophyll content.

4.1.1 Influence of chlorophyll content. The simulated position of the red-edge as a function of the leaf chlorophyll content for various LAI values is illustrated in figure 1. The red-edge shifts to longer wavelengths with increasing chlorophyll contents. Largest effects occur at the lower chlorophyll contents. This confirms the assumption that the red-edge index can be used as a measure for estimating the leaf chlorophyll content.

4.1.2 Influence of LAI. Figure 1 already showed that the LAI had a clear effect on the position of the red-edge index. The effect of varying LAI on simulated red-edge index for various leaf chlorophyll contents is presented in figure 2. The LAI has a significant influence on the red-edge position. There is a distinct shift of the red-edge to longer wavelength positions with increasing LAI. This shift is most pronounced at the lower LAI values.

4.1.3 Influence of soil background. As concluded before, one of the main advantages of working with the position of the red-edge is its insensitivity to soil background. Figure 3 illustrates the effect of soil reflectance on simulated values of the red-edge for varying LAI. Under the condition of our simulations, the position of the red-edge is not very sensitive to soil reflectance (spectrally constant soil reflectance) for a given LAI. The same is found as a function of chlorophyll content. A small shift to longer wavelengths occurs with increasing soil reflectance.

4.1.4 Atmospheric influence. Guyot et al. (1988) concluded from simulation studies that the position of the red-edge was unaffected by atmospheric conditions. This would be a second important characteristic of the red-edge (its independence of soil reflectance being the first one). Systematic errors in the atmospheric calibration of some spectral bands may have effects on the position of the red-edge. Moreover, bias in the reflectance measurements may cause false blue shifts that might be confused with real shifts because of vegetation stress (Bonham-Carter, 1988).

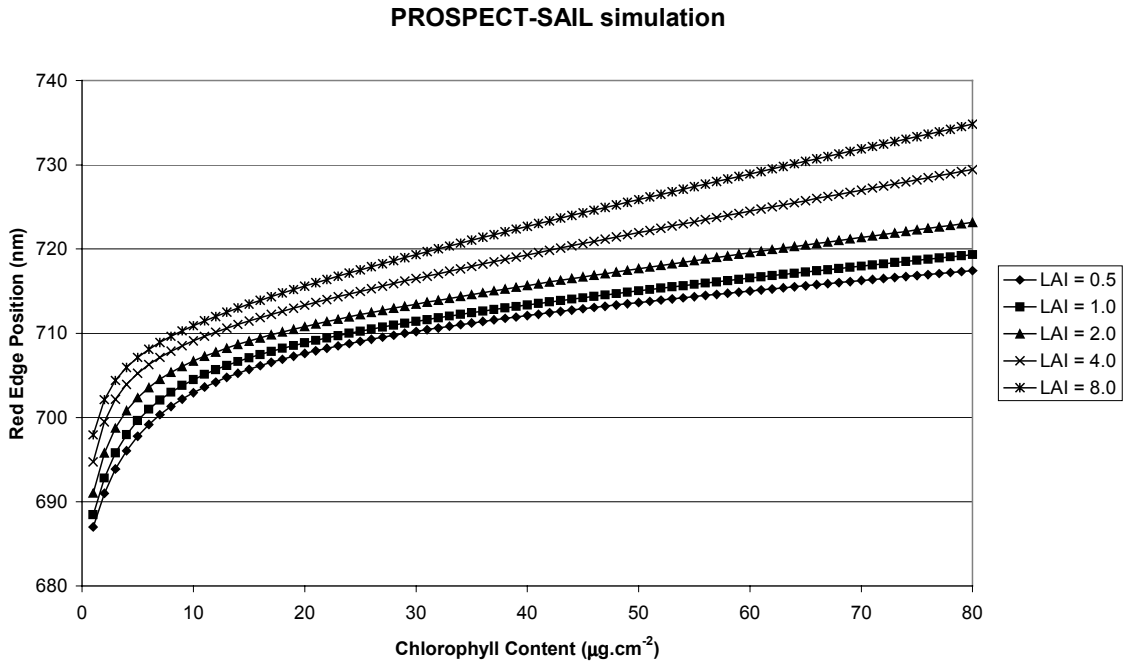

Figure 1. Influence of leaf chlorophyll content on simulated red-edge position for several LAI values of the standard crop. PROSPECT-SAIL simulation.

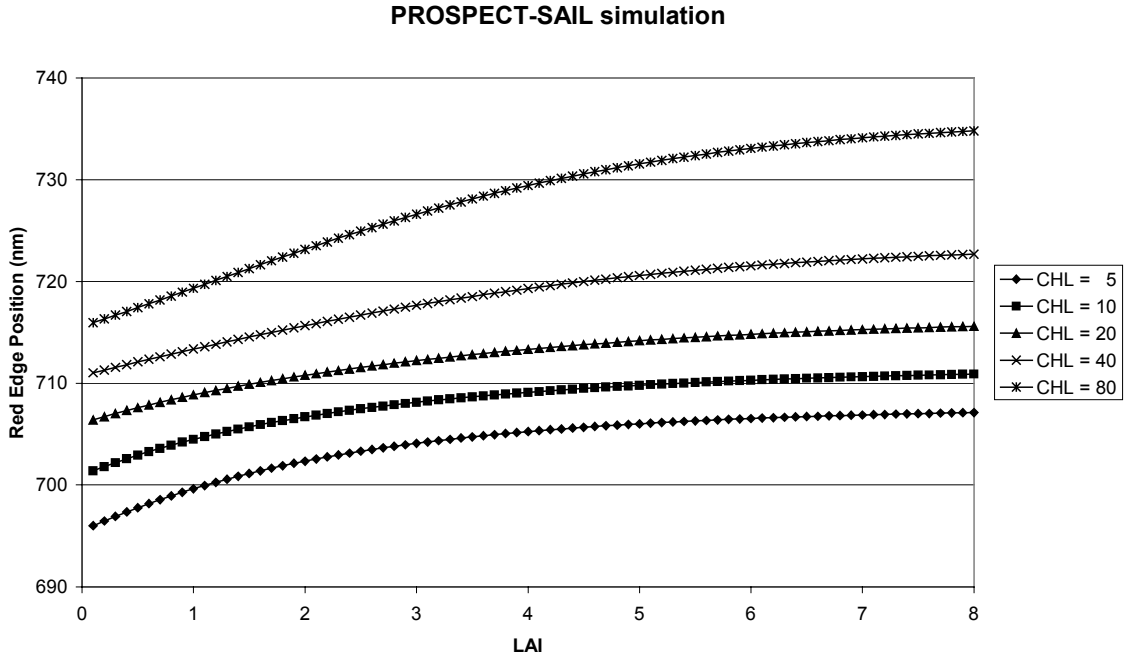

Figure 2. Influence of LAI on simulated red-edge position for various leaf chlorophyll contents (CHL in µg/cm²) of the standard crop. PROSPECT-SAIL simulation.

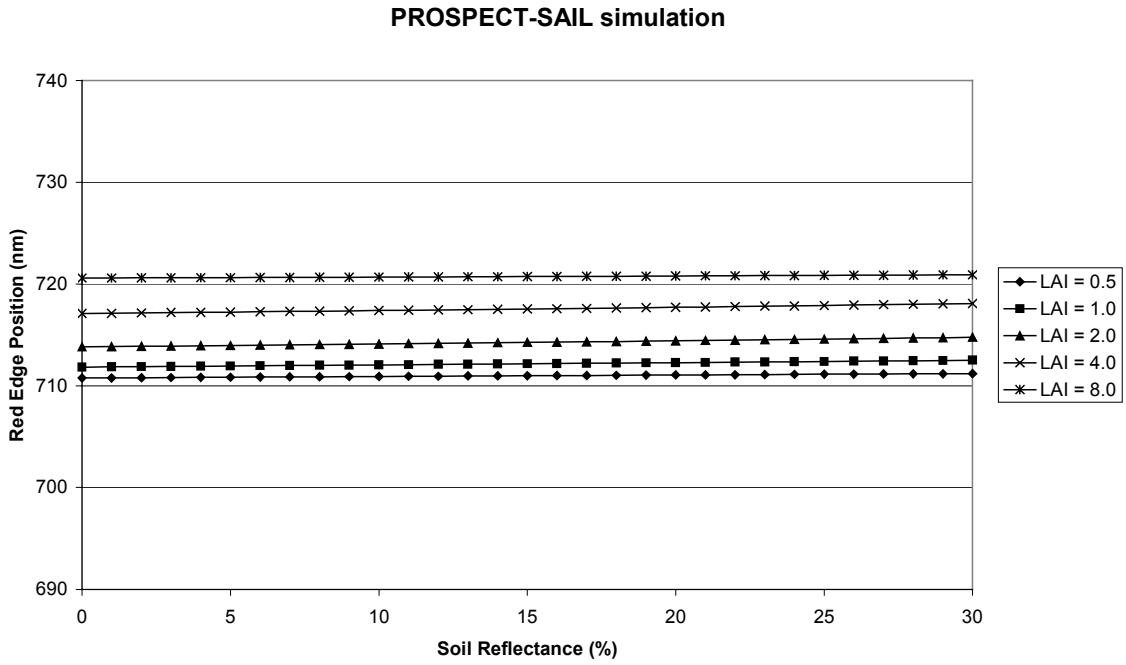

Figure 3. Influence of the soil reflectance on simulated red-edge position for various LAI values of the standard crop. PROSPECT-SAIL simulation.

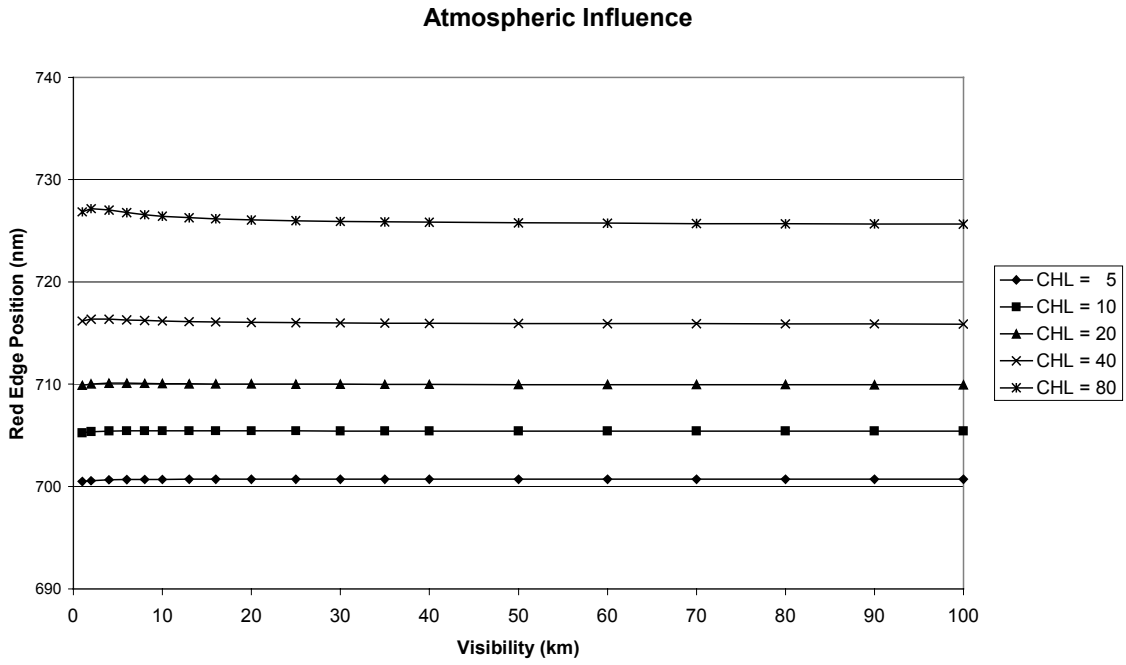

Figure 4. Influence of the atmospheric influence (in terms of visibility) on simulated red-edge position for various leaf chlorophyll contents (CHL in µg/cm²) of the standard crop. PROSPECT-SAIL simulation.

For calibration errors that are constant for a whole scene, systematic (but not constant) shifts of the position of the red-edge will be introduced, but local anomalies will be detectable. However, for multidate or interscene comparisons, calibration errors could produce misleading results.

The atmospheric influence in airborne or spaceborne measurements around the red-NIR slope is captured within the transformation from radiance values at the sensor (or digital numbers) to reflectances at ground level. Clevers and Buiten (1991) describe an atmospheric model based on the model of Richards (1986). However, they extended the model of Richards by including diffuse and direct upward fluxes in addition to the direct and diffuse downward fluxes. Moreover, they included multiple reflections between the earth's surface and the atmosphere. Results of the atmospheric correction procedure using this extended model in combination with parameterization methods of Iqbal (1983) yielded good results for the Flevoland study area in The Netherlands. Similar results were obtained using the model of Verhoef (1985a, 1985b, 1998).

The above atmospheric model was used for studying the influence of the atmosphere on the calculation of the red-edge index. The visibility is used as an indicator for the state of the atmosphere. Figure 4 depicts the influence of the atmosphere on the position of the red-edge for various chlorophyll contents. As expected, the influence of the atmosphere is only minor.

4.1.5 Other variables. The influence of other vegetation variables, like leaf structure, leaf size (hot-spot parameter) and leaf angle distribution, and of other external variables, like solar angle and diffuse/direct irradiation ratio, on the position of the red-edge index appear to be minor.

4.2. Red-edge index simulation with MERIS

4.2.1 AVIRIS spectra. Data set II comprises real imaging spectrometer measurements over an agricultural area. Figure 5 illustrates the radiance spectrum in the red-edge region for the main three crops in the area. For the "linear method" the following AVIRIS spectral bands can be employed: 667.4 – 697.3 – 736.7 – 785.0 nm. Clevers (1994) showed that the red-edge position determined from these radiance values was similar to the one obtained from spectral reflectance measurements performed in the field using a hand-held radiometer. Notable in figure 5 is a dip in the radiance curve at about 760 nm. This is a well-known absorption feature caused by oxygen present in the atmosphere. Also an absorption feature at about 820 nm, caused by water vapour in the atmosphere, is obvious. Since MERIS has a spectral band at about 753 nm, biased results can be expected in applying the "linear method" of Guyot when no atmospheric correction is performed.

Figure 6 illustrates the spectral signature in terms of reflectance for the main three crops in the area after an atmospheric correction has been performed. The oxygen absorption feature has been removed in this way.

4.2.2 MERIS simulations. As seen in table 1, MERIS has also a spectral band in the chlorophyll absorption feature at 665 nm and at the NIR plateau at 775 nm. These are very close to the wavelengths used in the "linear method" as described by Guyot and Baret (1988) and can be used for estimating the reflectance value at the inflexion point. The next step in the "linear method" is to translate this reflectance value at the inflexion point to the corresponding wavelength by a linear interpolation between the reflectances measured at two wavelength positions on the red-edge slope. From the MERIS standard band setting, the spectral bands centred at 705 and 753.75 nm are available. In this section it will be tested whether these bands yield useful estimates of the red-edge position. When the MERIS bands are simulated we will call the linear method the "MERIS method".

Using data set I, figure 7 illustrates the red-edge position as a function of the leaf chlorophyll content for the "linear method" using the interpolation between 700 and 740 nm and for the "linear method" using the MERIS band setting and interpolating between 705 and 754 nm. Both curves exhibit the same pattern, whereby the MERIS-based "linear method" shows somewhat larger red-edge index values, except for index values below 705 nm. For the latter range considerable deviations between the two methods may occur, which primarily can be attributed to the fact that using the MERIS bands we are performing an extrapolation instead of an interpolation. The relationship between the two methods is depicted in figure 8 for smaller steps in chlorophyll content and for canopies with various LAI values. It shows a good linear relationship in this case albeit that it not matches the 1:1 line. This result shows that one may derive one general relationship between the two methods and that a linear relationship will yield a good fit to the data. Using all the data of figure 8, the regression line yields:

$re_{MERIS} = -409.0 + 1.574 * re_{700-740}$

$r = 0.996$.

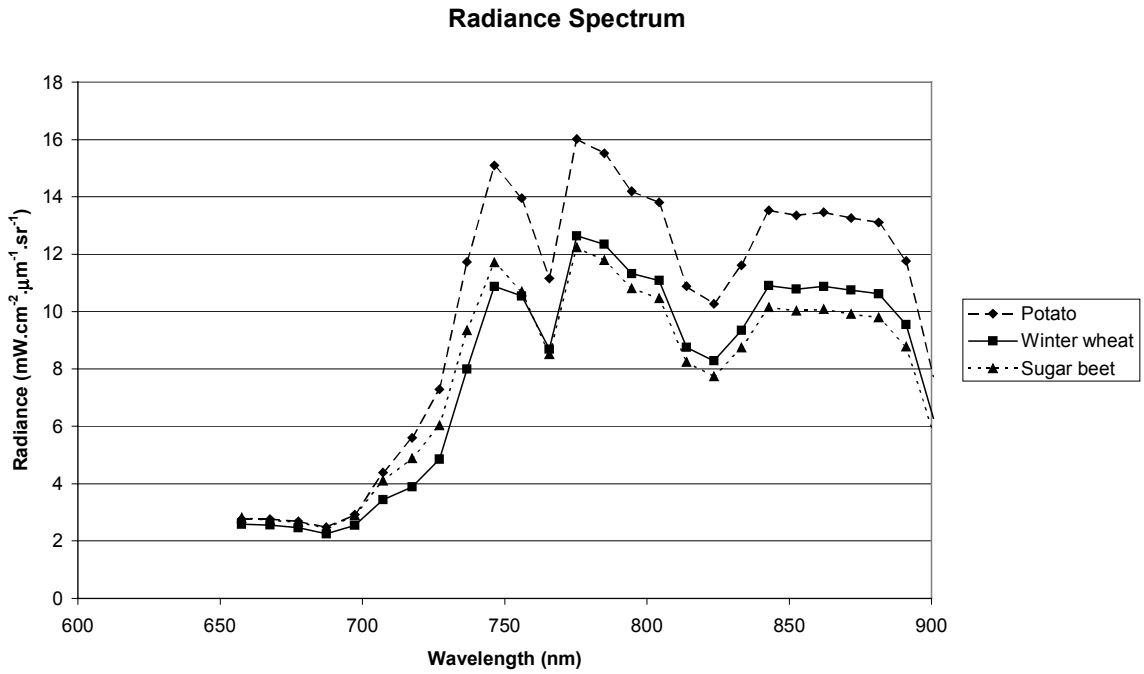

Figure 5. Spectral signature in radiance ($mW.cm^{-2}.\mu m^{-1}.sr^{-1}$) for the three major crops at the Flevoland test area, measured with the AVIRIS sensor on July 5th, 1991.

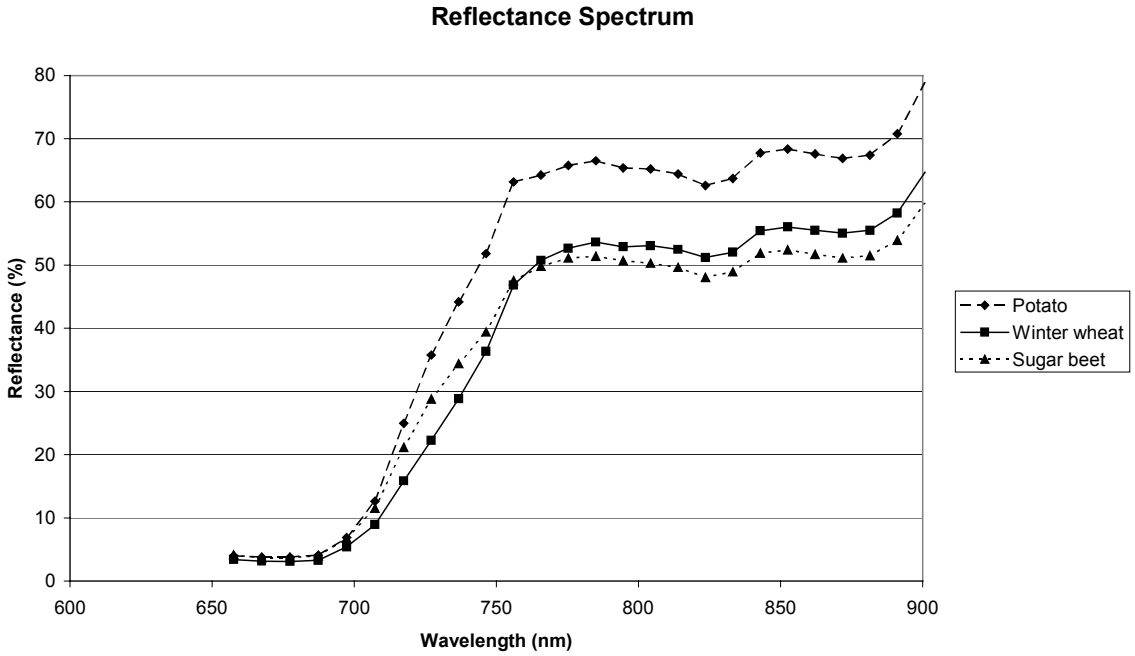

Figure 6. Spectral signature in terms of reflectance for the three major crops at the Flevoland test area, measured with the AVIRIS sensor on July 5th, 1991.

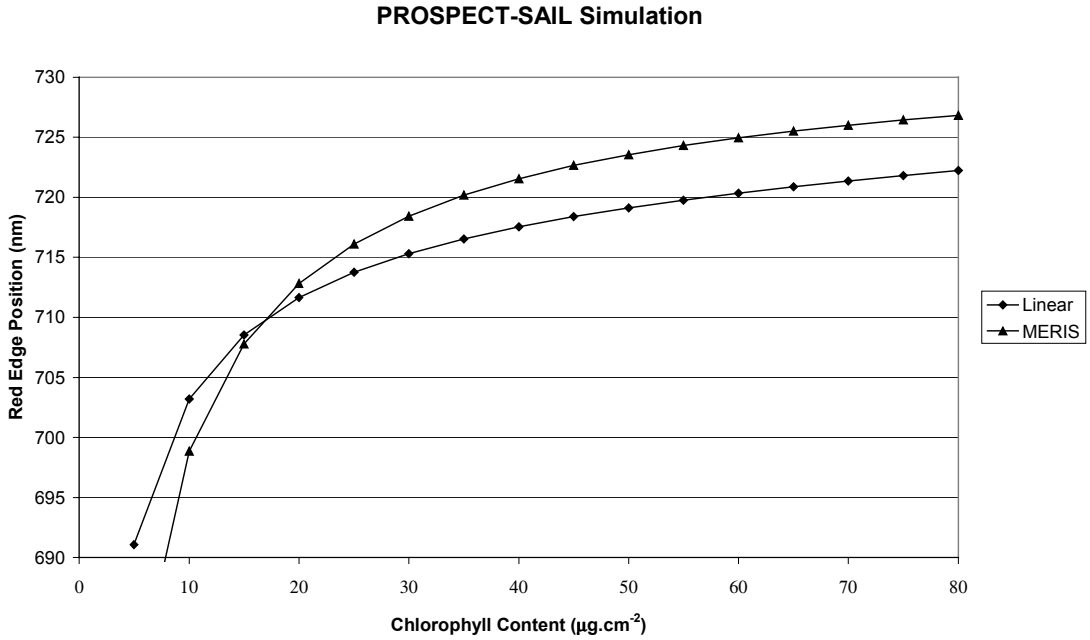

Figure 7. Red-edge position as a function of the leaf chlorophyll content for the "linear method" using the 700 and 740 spectral bands and for the linear method using the MERIS band setting ("MERIS method") for a canopy with an LAI of 2.0 as simulated with a combined PROSPECT-SAIL model.

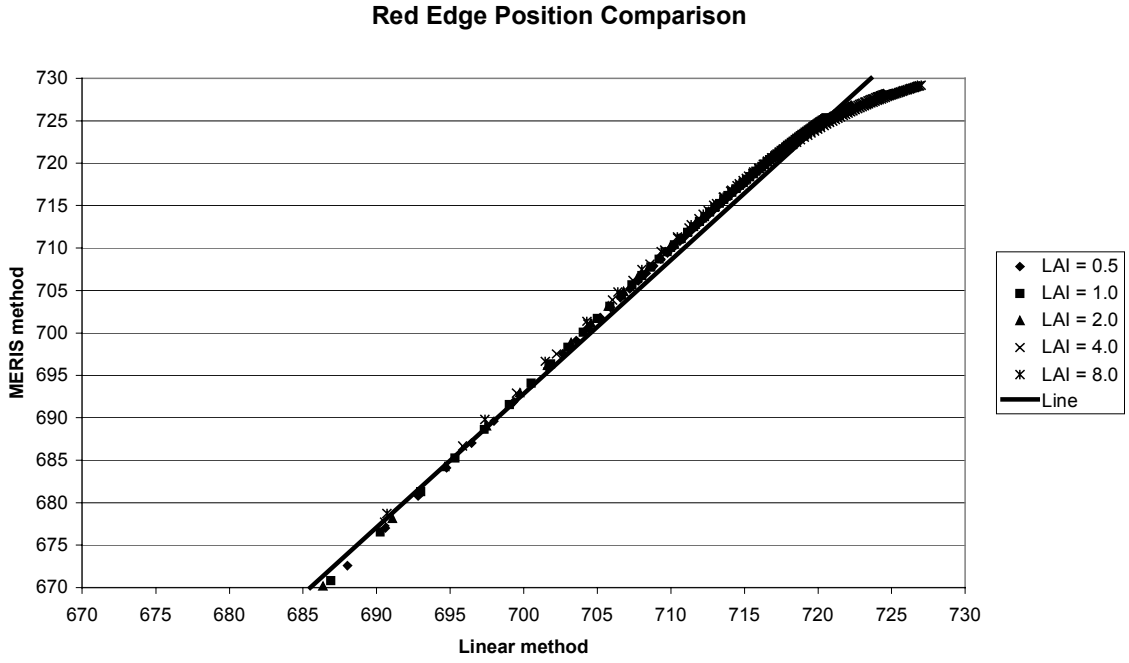

Figure 8. Comparison of the red-edge position calculated using the "linear method" interpolating between 700 and 740 nm and the "MERIS method", thus interpolating between 705 and 754 nm. PROSPECT-SAIL simulation for a canopy with varying leaf chlorophyll content and various LAI values.
The regression line $re_{MERIS} = -409.0 + 1.574 * re_{700\text{-}740}$ is also plotted.

Figure 9. Comparison of the red-edge position calculated using the "linear method" interpolating between 697 and 737 nm and the "MERIS method" for the main crops and bare soils at the Flevoland site, measured with the AVIRIS sensor on July 5th, 1991.
The regression line from figure 8 is also plotted.

Using data set II, MERIS spectral bands were simulated with the AVIRIS bands. The bands at 667 and 775 nm were used for estimating the reflectance at the inflexion point and the bands at 707 and the average of 746 and 756 nm were used for the linear interpolation. Figure 9 illustrates the relationship between the red-edge position calculated from the interpolation between 697 and 737 nm and that calculated using the simulated MERIS bands for the main agricultural crops at the Flevoland test site. When we compare this relationship with the regression line found for data set I, again a good match is observed. Like for the other data sets larger deviations occur at high red-edge values.

Results for both data sets show that there exists a nearly linear relationship for the "linear method" using either bands at about 700 and 740 nm or the MERIS bands, albeit that it not coincides with the 1:1 line. Actually, this means that we have to work with instrument-specific red-edge indices. For MERIS, the above-mentioned linear relationship may be used for translating red-edge index values obtained with one method (using the MERIS bands) into values obtained with the other method (based on bands at 700 and 740 nm). Deviations occur mainly at high red-edge index values matching vegetation with a high chlorophyll content and with very high LAI values. To cope with this a non-linear function might be fitted. Another possibility is to fit a second linear relationship for the upper part of the curve. The breakpoint then seems to lay at about 720 nm for the standard "linear method" (coinciding with about 725 nm for the "MERIS method"). When fitting a linear function for this upper part of the curve, the regression line yields:

$re_{MERIS} = -243.7 + 0.668 * re_{700-740}$

$r = 0.980$.

For the remaining part of the curve still the relationship given in the previous section will be used. The two regression lines are illustrated in figure 10 for data set I. When plotting these two regression lines with the results of data set II (figure 11) reasonable results are found, although the "MERIS method" underestimates the highest red-edge values in comparison to the regression line. It appears, moreover, that the determination of the red-edge index using the MERIS band setting becomes less sensitive to variations in chlorophyll content and LAI than the standard "linear method" using interpolation between 700 and 740 nm.

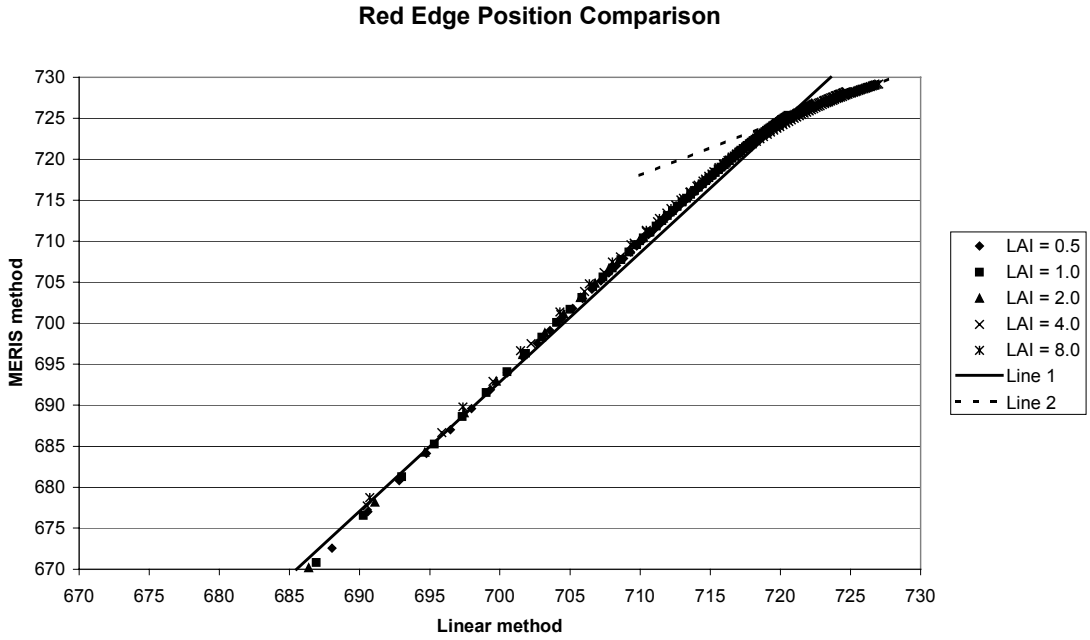

Figure 10. Comparison of the red-edge position calculated using the "linear method" interpolating between 700 and 740 nm and the "MERIS method", thus interpolating between 705 and 754 nm. PROSPECT-SAIL simulation for a canopy with varying leaf chlorophyll content and various LAI values.
The two regression are also plotted: Line 1: $re_{MERIS} = -409.0 + 1.574 * re_{700-740}$
Line 2: $re_{MERIS} = -243.7 + 0.668 * re_{700-740}$

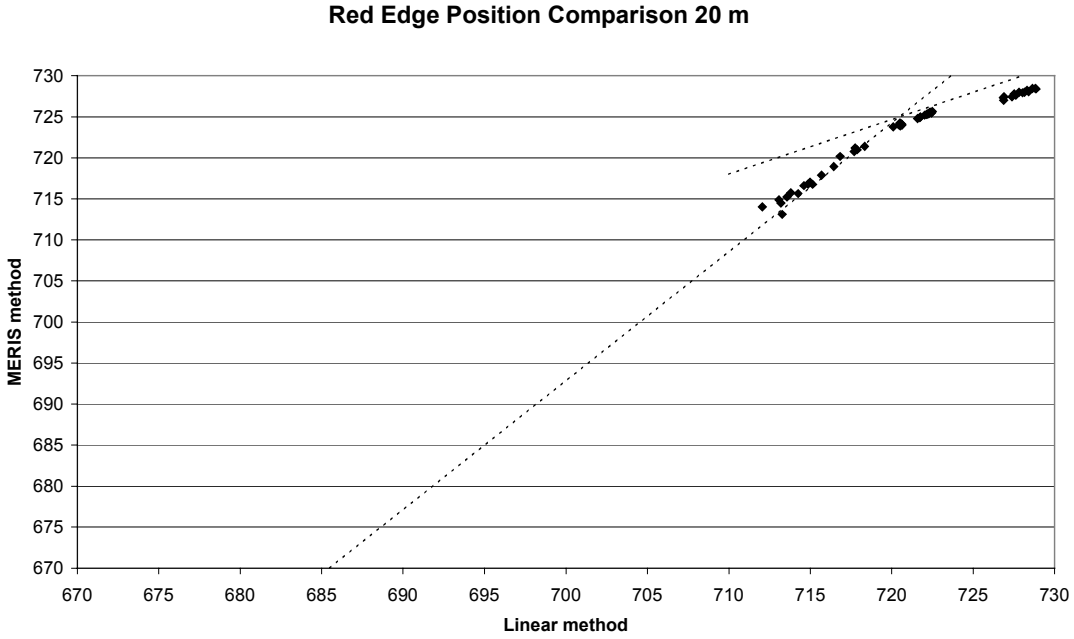

Figure 11. Comparison of the red-edge position calculated using the "linear method" interpolating between 697 and 737 nm and the "MERIS method" for the main crops at the Flevoland site, measured with the AVIRIS sensor on July 5th, 1991.
The regression lines from figure 10 are also plotted.

4.2.3 Upscaling to the MERIS resolution. In section 4.2.2 the red-edge index was calculated for the simulated MERIS bands using AVIRIS data at 20 m spatial resolution (cf. figure 11). A colour composite for the Flevoland test area is depicted in colour plate 1. MERIS pixels of 300 m spatial resolution were simulated by taking the average reflectance of 15 x 15 pixels for all AVIRIS spectral bands. The resulting colour composite is also depicted in colour plate 1. This image shows that we cannot recognize the individual agricultural fields anymore. However, when there are fields with high biomass (red colour in the image) close to each other, we recognize an area with high biomass (red MERIS pixel) in the spatially degraded image. The same is true, for instance, for areas with low or no vegetation cover (the bluish colours).

Figure 12 illustrates the relationship between the red-edge position calculated from the interpolation between 697 and 737 nm and that calculated using the simulated MERIS bands for a number of degraded pixels at the Flevoland test site. When we compare this relationship with the relationship found at 20 m spatial resolution (figure 11), we see that the data coincide very well and that the relationships match. The range in red-edge values at 300 m is less because there are no points at the lower end in comparison to the range at 20 m. This is caused by the fact that no pure bare soil points are present in the degraded image.

From this we may conclude that the red-edge index derived for the MERIS spectral bands at the MERIS spatial resolution of 300 m still provides useful information. If the objects at the earth surface are large enough, we may obtain a significant range in red-edge values. At the Flevoland agricultural test site individual fields could not be recognized, but MERIS will provide informative red-edge values on large units (groups of fields).

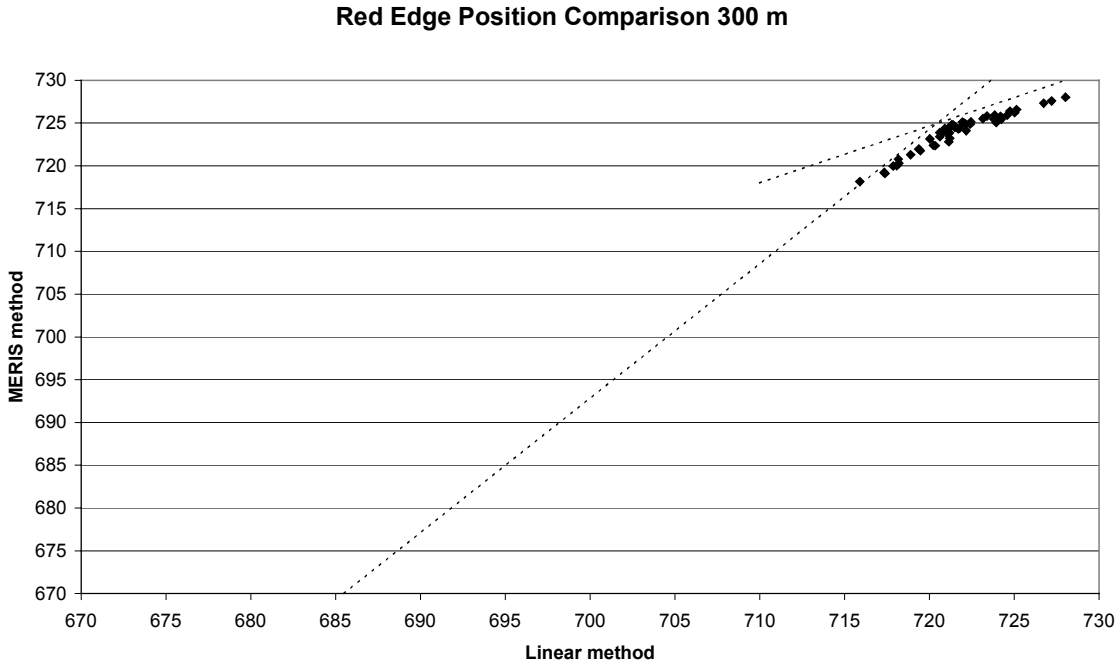

Figure 12. Comparison of the red-edge position calculated using the “linear method” interpolating between 697 and 737 nm and the “MERIS method” for AVIRIS pixels degraded to 300 m at the Flevoland site.
The regression lines from figure 10 are also plotted.

Colour Plate 1:

Top: Colour composite of AVIRIS spectral bands 44 (786 nm), 28 (667 nm) and 16 (549 nm) in RGB for the Flevoland test site, July 5th, 1991.

Bottom: Colour composite of AVIRIS spectral bands 44, 28 and 16 in RGB, resampled to 300 m, for the Flevoland test site, July 5th, 1991.

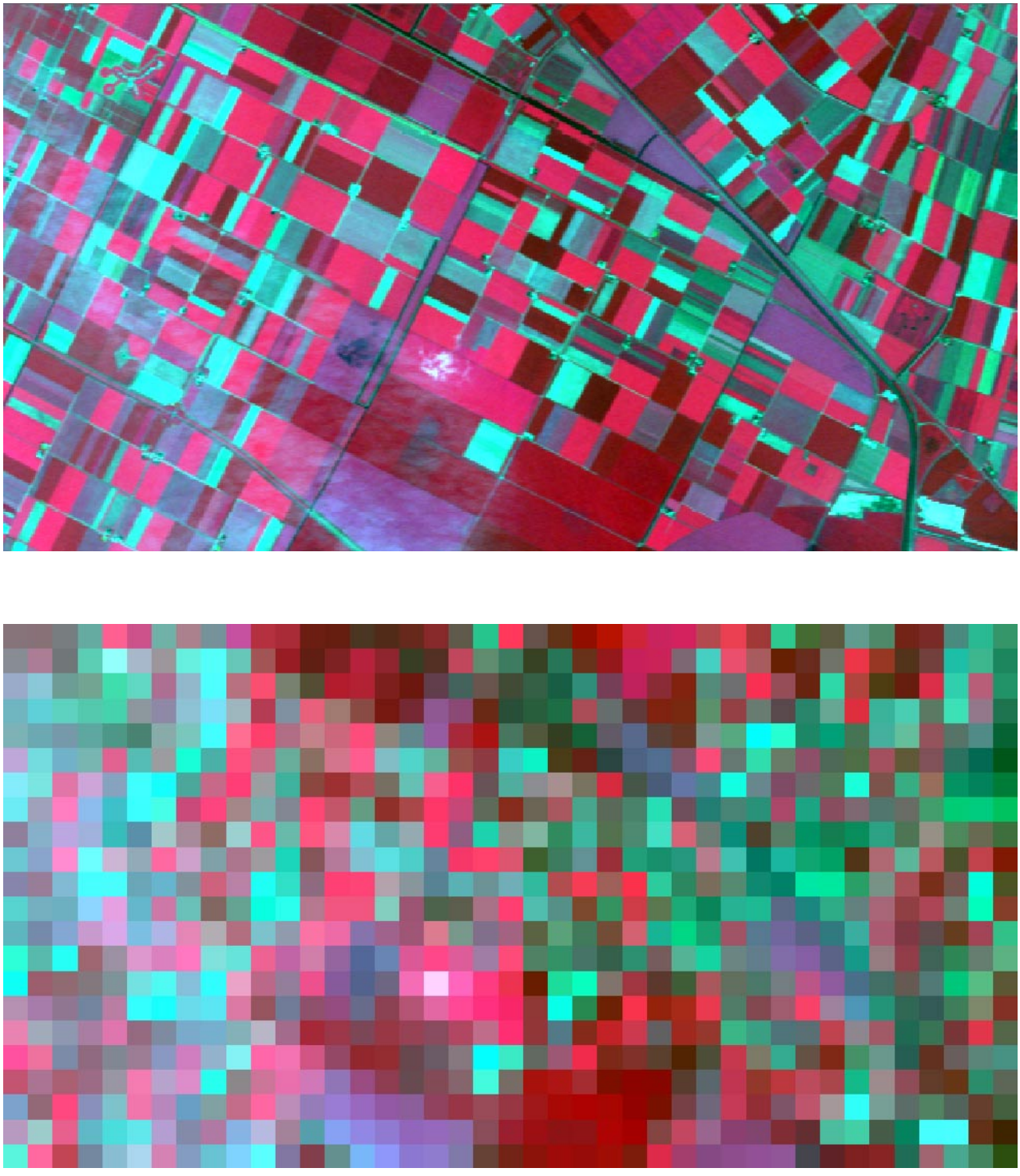

5. CONCLUSIONS

The “linear method” (Guyot and Baret, 1988) assumes a straight slope of the reflectance spectrum around the midpoint between the reflectance at the NIR plateau and the reflectance minimum at the chlorophyll absorption feature in the red. This midpoint is then defined as the red-edge index. This point may not coincide with the maximum of the first derivative, but it appears to be a very robust definition and it needs only a very limited number of spectral bands. Thus, this method is very useful for practical applications.

The red-edge index may be considered as a particular "vegetation index" of interest because of its low sensitivity to disturbing factors such as atmospheric conditions or soil brightness and its high sensitivity to canopy characteristics such as chlorophyll content or LAI.

Although the spectral bands of the MERIS standard band setting at the red-edge slope are not optimally located, they can be used for applying the “linear method” for red-edge index estimation. The bands to be used are located at 705 and 753.75 nm. However, since the latter band is located very close to the oxygen absorption feature of the atmosphere, an atmospheric correction must be applied previous to calculating the position of the red-edge using the MERIS bands. Previous studies (e.g., Clevers, 1994) have shown that for bands located at about 700 and 740 nm, an atmospheric correction is not necessary since the red-edge calculated in terms of reflectances equals the one calculated in terms of radiances.

The red-edge index derived for the MERIS spectral bands at the MERIS spatial resolution of 300 m still provides useful information. If the objects at the earth surface are large enough, we may obtain specific information concerning these objects.

ACKNOWLEDGEMENTS

We acknowledge partial financial support by the Netherlands Remote Sensing Board (BCRS contract 3.1/AP-07).

REFERENCES

Allen, W.A., Gausman, H.W., Richardson, A.J. and Thomas, J.R., 1969. Interaction of isotropic light with a compact plant leaf. Journal of the Optical Society of America, 59, 1376-1379.

Allen, W.A., Gausman, H.W., and Richardson, A.J., 1970. Mean effective optical constants of cotton leaves. . Journal of the Optical Society of America, 60, 542-547.

Bonham-Carter, G.F., 1988. Numerical procedures and computer program for fitting an inverted gaussian model to vegetation reflectance data. Computers and Geosciences, 14, 339-356.

Büker, C., and Clevers, J.G.P.W., 1992. Imaging spectroscopy for agricultural applications. Report LUW-LMK-199206, Dept. Landsurveying and Remote Sensing, Wageningen Agricultural University, The Netherlands.

Bunnik, N.J.J., 1978. The multispectral reflectance of shortwave radiation by agricultural crops in relation with their morphological and optical properties. PhD Thesis, Mededelingen Landbouwhogeschool Wageningen 78-1, Wageningen, The Netherlands.

Clevers, J.G.P.W., 1994. Imaging spectrometry in agriculture - Plant vitality and yield indicators. In Imaging Spectrometry - A Tool for Environmental Observations, edited by J. Hill and J. Mégier (Dordrecht: Kluwer Academic), pp. 193-219.

Clevers, J.G.P.W., 1999. The use of imaging spectrometry for agricultural applications. ISPRS Journal of Photogrammetry and Remote Sensing, 54, 299-304.

Clevers, J.G.P.W., and Buiten, H.J., 1991. Multitemporal analysis of optical satellite data. BCRS, Delft, report 91-02, 64 pp.

Clevers, J.G.P.W., and Büker, C., 1991. Feasibility of the red edge index for the detection of nitrogen deficiency. Proceedings 5th Int. Coll. "Physical Measurements and Signatures in Remote Sensing", Courchevel, France, ESA SP-319, pp. 165-168.

Clevers, J.G.P.W., and Verhoef, W., 1993. LAI estimation by means of the WDVI: a sensitivity analysis with a combined PROSPECT-SAIL model. Remote Sensing Reviews, 7, 43-64.

Dawson, T.P., and Curran, P.J., 1998. A new technique for interpolating the reflectance red edge position. International Journal of Remote Sensing, 19, 2133-2139.

Demetriades-Shah T.H., and Steven, M.D., 1988. High spectral resolution indices for monitoring crop growth and chlorosis. Proceedings 4th Int. Coll. “Spectral Signatures of Objects in Remote Sensing”, Aussois, France, ESA SP-287, pp. 299-302.

Demetriades-Shah T.H., Steven, M.D., and Clark, J.A., 1990. High resolution derivative spectra in remote sensing. Remote Sensing of Environment, 33, 55-64.

Elvidge, C.D., 1990. Visible and near infrared reflectance characteristics of dry plant materials. International Journal of Remote Sensing, 11, 1775-1795.

ESA, 1995. MERIS: The Medium Resolution Imaging Spectrometer. Report SP-1184, ESA, Paris.

ESA, 1997. Envisat-1 Mission & System Summary. Report ESTEC-ESA, Noordwijk, The Netherlands.

Goel, N.S., 1989. Inversion of canopy reflectance models for estimation of biophysical parameters from reflectance data. In Theory and Applications of Optical Remote Sensing, edited by G. Asrar, (New York: Wiley), pp. 205-251.

Govaerts, Y.M., Verstraete, M.M., Pinty, B., and Gobron, N., 1999. Designing optimal spectral indices: a feasibility and proof of concept study. International Journal of Remote Sensing, 20, 1853-1873.

Guyot, G., and Baret, F., 1988. Utilisation de la haute resolution spectrale pour suivre l'etat des couverts vegetaux. Proceedings 4th Int. Coll. “Spectral Signatures of Objects in Remote Sensing”, Aussois, France, ESA SP-287, pp. 279-286.

Guyot, G, Baret, F., and Major, D.J., 1988. High spectral resolution: determination of spectral shifts between the red and near infrared. Int. Arch. of Photogr. and Rem. Sensing, 27(11), 750-760.

Horler, D.N.H., Dockray, M., and Barber, J., 1983. The red edge of plant leaf reflectance. International Journal of Remote Sensing, 4, 273-288.

Iqbal, M., 1983. An introduction to solar radiation. Academic Press, Ontario, Canada, 390 pp.

Jacquemoud S., and Baret, F., 1990. PROSPECT: a model of leaf optical properties spectra. Remote Sensing of Environment, 34, 75-91.

Rast, M., and Bézy, J.L., 1990. ESA’s Medium Resolution Imaging Spectrometer (MERIS): mission, system and applications. SPIE Journal, 1298, 114-126.

Rast, M., Bézy, J.L., and Bruzzi, S., 1999. The ESA Medium Resolution Imaging Spectrometer MERIS – a review of the instrument and its mission. International Journal of Remote Sensing, 20, 1681-1702.

Richards, J.A., 1986. Remote Sensing Digital Image Analysis: An introduction. Springer-Verlag, Berlin.

Van Den Bosch, J., and Alley, R., 1990. Application of LOWTRAN 7 as an atmospheric correction to Airborne Visible/Infrared Imaging Spectrometer (AVIRIS) data. In Proceedings of the second Airborne Visible/Infrared Imaging Spectrometer (AVIRIS) Workshop, edited by R.O. Green (Pasadena: JPL), JPL-Publication 90-54, pp. 78-81.

Verhoef, W., 1984. Light scattering by leaf layers with application to canopy reflectance modelling: the SAIL model. Remote Sensing of Environment, 16, 125-141.

Verhoef, W., 1985a. Earth observation modeling based on layer scattering matrices. Rem. Sens. Envir., 17, 165-178.

Verhoef, W., 1985b. A scene radiation model based on four stream radiative transfer theory. Proceedings 3rd International Colloquium on Spectral Signatures of Objects in Remote Sensing, Les Arcs, France, ESA SP-247, pp. 143-150.

Verhoef, W., 1998. Theory of radiative transfer models applied in optical remote sensing of vegetation canopies. PhD Thesis, Wageningen Agricultural University, The Netherlands, 310 pp.

Verhoef, W., and Bunnik, N.J.J., 1981. Influence of crop geometry on multispectral reflectance determined by the use of canopy reflectance models. Proceedings Int. Coll. “Signatures of Remotely Sensed Objects”, Avignon, France, pp. 273-290.

Verstraete, M.M., Pinty, B., and Curran, P.J., 1999. MERIS potential for land applications. International Journal of Remote Sensing, 20, 1747-1756.

Wessman, C.A., 1994. Estimating canopy biochemistry through imaging spectrometry. In Imaging Spectrometry - A Tool for Environmental Observations, edited by J. Hill and J. Mégier (Dordrecht: Kluwer Academic), pp. 57-69.